J|A|C|S
ARTICLES
Published on Web 05/10/2006

Indirect NMR Spin−Spin Coupling Constants ^3J(P,C) and ^2J(P,H) across the P−O···H−C Link Can Be Used for Structure Determination of Nucleic Acids

Vladimír Sychrovský,*[,†,‡] Jiří Šponer,[†,‡] Lukáš Trantírek,[§] and Bohdan Schneider[†]

Contribution from the Institute of Organic Chemistry and Biochemistry, Academy of Sciences of the Czech Republic, Flemingovo n. 2., 166 10 Praha 6, Czech Republic, Institute of Biophysics, Academy of Sciences of the Czech Republic, Královopolská 135, 612 65 Brno, Czech Republic, and Faculty of Biological Sciences, University of South Bohemia and Institute of Parasitology Academy of Sciences of the Czech Republic, Branišovská 31, 370 05 České Budějovice, Czech Republic

Received July 28, 2005; Revised Manuscript Received April 11, 2006; E-mail: vladimir.sychrovsky@uochb.cas.cz

Abstract: Calculated indirect NMR spin−spin coupling constants ^3J(P,C) and ^2J(P,H) were correlated with the local structure of the P−O···H−C linkage between the nucleic acid (NA) backbone phosphate and the H−C group(s) of a nucleic acid base. The calculations were carried out for selected nucleotides from the large ribosomal subunit (Ban et al. *Science* **2000**, *289*, 905) with the aim of identifying NMR parameters suitable for detection of certain noncanonical RNA structures. As calculations in the model system, dimethylphosphate−guanine, suggest, the calculated indirect spin−spin couplings across the linkage are sensitive to the mutual orientation and distance between the phosphate and nucleic acid base. A short distance between the nucleic acid base and phosphate group and the angles C···P−O and P···C−H smaller than 50° are prerequisites for a measurable spin−spin interaction of either coupling ($|J| > 1$ Hz). A less favorable arrangement of the P−O···H−C motif, e.g., in nucleotides of the canonical A-RNA, results in an effective dumping of both spin−spin interactions and insignificant values of the NMR coupling constants. The present work indicates that quantum chemical calculations of the indirect spin−spin couplings across the P−O···H−C motif can help detect some rare but important backbone topologies, as seen for example in the reverse kink-turn. Measuring of ^3J(P,C) and ^2J(P,H) couplings can therefore provide critical constraints on the NA base and phosphate geometry and help to determine the structure of NAs.

Introduction

Biological functions of nucleic acids (NAs) range from storing genetic information[1] to proteosynthesis.[2] These diverse functions require an equally diverse array of structures. The most biologically important DNA form is the B-DNA duplex,[3] a rather uniform double helix with standard Watson−Crick base pairs, modest sequence-dependent conformational variability at the base pair step level, and a uniform albeit rather flexible backbone. Besides the double helix, DNA can also adopt established noncanonic forms such as triplexes and quadruplexes.[4] The basic principles of three-dimensional organization of functional RNAs are strikingly different from DNA. The Watson−Crick (W−C) interactions, although still prevalent, no longer dominate. Atomic-resolution structures of RNAs have revealed that the nominally unpaired loop regions of RNAs are in fact involved in highly versatile non-W−C base pairing patterns that determine biochemical roles, evolution, and folding of RNA molecules.[5]

An astonishing diversity of molecular interactions in RNAs is accompanied by a wide variability of their conformations. This structural variability is, to a certain limit, restricted by possible conformations of the sugar−phosphate backbone which are further interrelated with the richness of the non-W−C interactions. At a dinucleotide level, a few dozens of distinct RNA backbone classes or families were already identified.[6] Non-W−C interactions stabilize tertiary contacts between remote segments of the RNAs and form specific non-W−C regions called RNA motifs. A limited number of repeating structural motifs are known such as the kink-turn motifs [7] or A-minor tertiary interactions.[8] These motifs are used in a modular way

[†] Institute of Organic Chemistry and Biochemistry, Academy of Sciences of the Czech Republic.
[‡] Institute of Biophysics, Academy of Sciences of the Czech Republic.
[§] University of South Bohemia and Institute of Parasitology Academy of Sciences of the Czech Republic.

(1) Luger, K. and Richmond, T. J. *Curr. Opin. Struct. Biol.* **1998**, *8*, 33−40.
(2) Ramakrishnan, V. *Cell* **2002**, *108*, 557−572.
(3) Drew, H. R.; Wing, R. M.; Takano, T.; Broka, C.; Tanaka, S.; Itakura, K.; Dickerson, R. E. *Proc. Natl. Acad. Sci. U.S.A.* **1981**, *78*, 2179−2183.
(4) (a) Haider, S. M.; Parkinson, G.; Neidle, S. *J. Mol. Biol.* **2002**, *320*, 189−200. (b) Gehring, K.; Leroy, J. L.; Gueron, M. *Nature* **1993**, *363*, 561−565. (c) Chen, L.; Cai, L.; Zhang, X.; Rich, A. *Biochemistry* **1994**, *33*, 13540−13546.
(5) Leontis, N. B.; Westhof, E. *RNA* **2001**, *7*, 499−512.
(6) (a) Murray, L. J. W.; Arendall, W. B., III; Richardson, D. C.; Richardson, J. S. *Proc. Natl. Acad. Sci. U.S.A.* **2003**, *100*, 13904−13909. (b) Schneider, B.; Morávek, Z.; Berman, H. M. *Nucleic Acids Res.* **2004**, *32*, 1666−1677.
(7) (a) Klein, D. J.; Schmeing, T. M.; Moore, P. B.; Steitz, T. A. *EMBO J.* **2001**, *20*, 4214−4221. (b) Leontis, N. B.; Westhof, E. *Curr. Opin. Struct. Biol.* **2003**, *13*, 300−308.

to build uniquely folded structures of RNA molecules and to perform different structural and functional roles.

Seemingly unusual interactions and backbone topologies may be of key importance in some noncanonical motifs, and their accurate and unambiguous description via atomic-resolution experimental methods is necessary for a proper understanding of the structural variability and folding of RNA molecules. Among various methods for determination of NA structure, NMR spectroscopy plays an indispensable role; structures determined by NMR methods represent about half of all naked nucleic acids deposited in the NDB.[9] Although the sugar−phosphate backbone is key for determination of the NA structures, its conformations are difficult to determine by NMR methods. Difficulties arise from the structural complexity of the backbone, its relatively low proton density, and technical problems with acquiring and interpretation of the heteronuclear data. Any independent structural information about the backbone is therefore of great importance especially when the noncanonical NA structural motifs are investigated.

Recently, several new NMR methods have been introduced for determination of the phosphate backbone conformations using residual dipolar couplings,[10] cross-correlated relaxation between dipole−dipole and chemical shift anisotropy,[11] and P chemical shift offset.[10b,c,12] Use of calculated scalar coupling constants for structural validation across a variety of noncovalent links has been reviewed recently.[13]

Indirect spin−spin couplings across the phosphate P−O bond and the H−C bond of a nucleotide base in the P−O···H−C motif was, to the best of our knowledge, analyzed for the first time in this study. We show that predicted NMR spin−spin couplings can be used for detection of certain P−O···H−C motifs and further determination of their geometries. We determined how calculated indirect NMR spin−spin coupling constants ^3J(P,C) and ^2J(P,H) correlate with a local topology of the P−O···H−C motif. The motif is not detectable in the canonical A- or B-type double helical forms by the above NMR couplings. However, certain well-established RNA backbone structural classes (rotamers)[6] as well as some rare structural motifs can adopt conformations with measurable values of the scalar spin−spin couplings across their P−O···H−C link.

Calculation Method

The DFT B3LYP method and 6-31G** basis set were used in the optimization of molecular geometry. Indirect NMR spin−spin coupling constants were calculated using the Coupled Perturbed DFT method[14] with the B3LYP functional by including the diamagnetic spin−orbit (DSO), paramagnetic spin−orbit (PSO), Fermi-contact (FC) and spin−dipolar (SD) terms.[15] Among the tested DFT functionals the B3LYP functional was found to fit the experimental couplings best.[14a,14b] Therefore we used the B3LYP functional for calculation of spin−spin couplings in this work. The calculation of spin−spin couplings in the model system was performed on the geometry grid with the atomic basis usually called IglоII.[16] To ensure the convergence of calculated spin−spin couplings, several calculations were performed with the IglоII basis and the larger basis usually called Iglo III[16] in selected nucleotides. The basis set Iglo II was used for actual calculation in RNA nucleotides. The effect of water solvent was calculated with the Polarized Continuum Model (PCM).[17] All calculations were done with the G03 program package.[18]

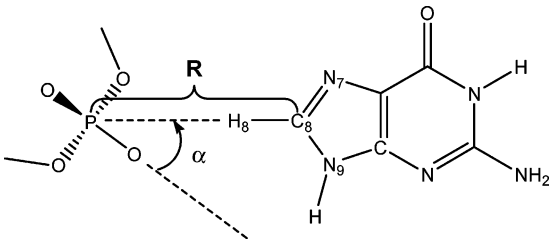

Figure 1. Model complex of dimethyl-phosphate in interaction with the guanine base. The interatomic distance *R* and angle α were used as geometry parameters in grid point calculations.

Results and Discussion

Calculation of a Model Complex. The ^3J(P,C) and ^2J(P,H) coupling constants were first calculated as a function of geometry of the P−O···H−C link in an idealized complex of guanine base interacting with dimethyl-phosphate (G···dmP), the complex is schematically shown in Figure 1. The geometry of monomer units, guanine and dimethyl-phosphate, was first optimized separately. The complex was than fixed with the linear arrangement of the P−O···H−C atoms, and only the interatomic distance between carbon and phosphorus of the P−O···H−C link was optimized while keeping the rest of the geometry parameters fixed. The model structure of the G···dmP complex thus corresponds to the energy minimum for the P−C interatomic distance under the P−O···H−C linearity constraint without relaxation of monomers. A series of spin−spin coupling constants was calculated for geometries of the two-dimensional grid formed by the interatomic distance between phosphorus and carbon (R(P···C)) and the angle C···P−O, as depicted in Figure 1. The interatomic distance R(H···O) varies as shown in Figure 2 since the linear arrangement of atoms C, H, and P as well as the rest of the geometry parameters of the G···dmP complex is kept fixed in all grid points. All geometry parameters were only varied on the grid without any geometry optimization.

The dependence of the calculated coupling constants ^3J(P,C) and ^2J(P,H) on the geometry of the P−O···H−C link in the G···dmP complex is shown in Figure 3. The sign of the ^3J(P,C) coupling is positive for the angle C···P−O at 0°, 10°, and 30°, while for the angle C···P−O at 50° and 90° it is negative due

(8) (a) Nissen, P.; Ippolito, J. A.; Ban, N.; Moore, P. B.; Steitz, T. A. *Proc. Natl. Acad. Sci. U.S.A.* **2001**, *98*, 4899−4903. (b) Moore, P. B.; Steitz, T. A. *Annu. Rev. Biochem.* **2003**, *72*, 813−850. (c) Ogle, J. M.; Carter, A. P.; Ramakrishnan, V. *Trends Biochem. Sci.* **2003**, *28*, 259−266.
(9) Berman, H. M.; Olson, W. K.; Beveridge, D.; Westbrook. J.; Gelbin, A.; Demeny, T.; Shieh, S.-H.; Srinivasan, A. R.; Schneider, B. *Biophys. J.* **1992**, *63*, 751−759.
(10) (a) Henning, M.; Carlomagno, T.; Williamson, J. R. *J. Am. Chem. Soc.* **2001**, *123*, 3395−2296. (b) Tjandra, N.; Tate, S.; Ono, A.; Kainosho, M.; Bax, A. *J. Am. Chem. Soc.* **2000**, *122*, 6190−6200. (c) Wu, Z.; Delaglio, F.; Tjandra, N.; Zhurkin, V. B.; Bax, A. *J. Biomol NMR.* **2003**, *26*, 297−315. (d) Grzesiek, S.; Cordier, F.; Jaravine, V.; Barfield, M. *Prog. NMR Spectrosc.* **2004**, *45*, 275−300.
(11) (a) Richter, C.; Reif, B.; Griesinger, C.; Schwalbe, H. *J. Am. Chem. Soc.* **2000**, *122*, 12728−12731. (b) Schwalbe, H.; Carlomagno, T.; Hennig, M.; Junker, J.; Reif, B.; Richter, C.; Griesinger, C. *Methods Enzymol.* **2001**, *338*, 35−81.
(12) Wu, Z.; Tjandra, N.; Bax, A. *J. Am. Chem. Soc.* **2001**, *123*, 3617−3618.
(13) Alkorta, I.; Elguero, J. *Int. J. Mol. Sci.* **2003**, *4*, 64−92.
(14) (a) Sychrovský, V.; Gräfenstein, J.; Cremer, D. *J. Chem. Phys.* **2000**, *113*, 3530−3547. (b) Helgaker, T.; Watson, M.; Handy, N. C. *J. Chem. Phys.* **2000**, *113*, 9402−9409. (c) Barone, V.; Peralta, J. E.; Contreras, R. H.; Snyder, J. P. *J. Phys. Chem. A* **2002**, *106*, 5607−5612.
(15) (a) Ramsey, N. F.; *Phys. Rev.* **1953**, *91*, 303−307. (b) Helgaker, T.; Pecul, M. In *Calculation of NMR and EPR properties*; Kaupp, M., Ed.; Wiley: 2002.
(16) Kutzelnigg, W.; Fleischer, U.; Schindler, M. In *NMR−Basis Principles and Progress*; Springer: Heidelberg, 1990; p 165.
(17) (a) Cossi, M.; Rega. N.; Scalmani, G.; Barone, V. *J. Comput. Chem.* **2003**, *24*, 669−681. (b) Klamt, A.; Eckert, F.; Hornig, M.; Beck, M. E.; Burger, T. *J. Comput. Chem.* **2002**, *23*, 275−281.
(18) Frisch, M. J. et al. *Gaussian 03*, revision C.02; Gaussian, Inc.: Wallingford, CT, 2004.

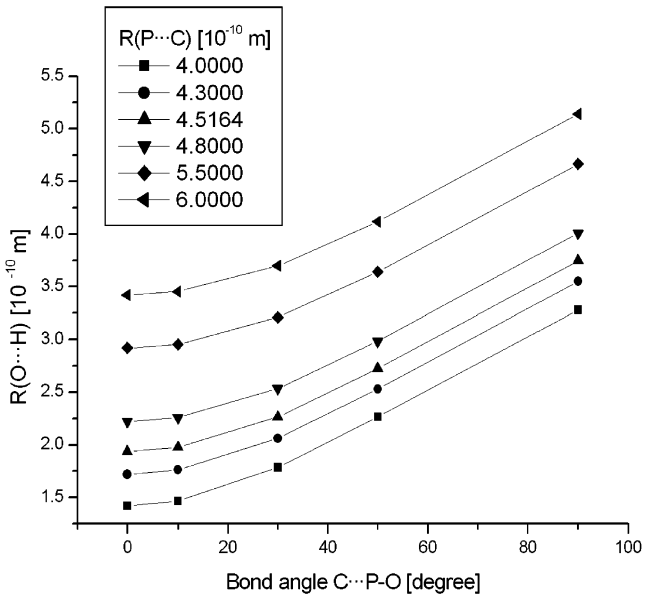

Figure 2. Variation of interatomic distance between oxygen and hydrogen R(O···H) as a function of the angle C···P−O in the P−O···H−C motif in the grid point calculations in the model complex G···dmP.

to the sign flip of the Fermi-contact contribution (see the Supporting Information). The ^2J(P,H) coupling is negative for the angle C···P−O at 0° ÷ 30°, while for the grid points of 50° and 90° a positive value was also calculated due to the Fermi-contact term similar to the case for the ^3J(P,C) coupling. Both couplings apart from their sign show very similar dependence on the geometry descriptors of the angle C···P−O and the interatomic distance R(P···C). The analytical fit discussed in detail in the Appendix (see Supporting Information) can be used for the qualitative correspondence of both J couplings with the molecular structure of real nucleotides as presented in the following section.

Both couplings decay rapidly to zero with increasing C···P−O angle and elongating interatomic distance R(P···C). The values of ^3J(P,C) and ^2J(P,H) couplings were 15.3 and −3.1 Hz, respectively, assuming the optimal geometry of the G···dmP complex (R(P···C) = 4.52 Å, R(O···H) = 1.94 Å) and the zero value of angle C···P−O. The ^3J(P,C) and ^2J(P,H) couplings decrease to 2.4 and −0.33 Hz, respectively, when the angle C···P−O is just 30° off the linear arrangement keeping the optimal P···C and O···H distances (R(P···C) = 4.52 Å, R(O···H) = 2.26 Å). The absolute values of both NMR couplings are smaller than 1 Hz when the C···P−O angle reaches a value close to 50° and larger even upon close contact of the monomer units. For the grid point geometry with the interatomic distance R(P···C) equal to 4.00 Å and the C···P−O angle 50.0°, the absolute value of both couplings was smaller than 0.1 Hz although the distance R(O···H) was short, 2.27 Å. Rapid decrease of both NMR couplings with increasing deviation from collinearity of P−O and H−C bonds at any given interatomic distance R(P···C) is further enhanced by the simultaneous increase of the R(O···H) interatomic distance as shown in Figure 2.

A similar strong damping of the NMR couplings has been observed experimentally in the P−O···H−N linkage by Shirakawa et al.[19] and later confirmed theoretically by Czernek and Bruschweiler;[20a] the corresponding coupling, ^3J(P,N), is modulated by an analogical angle, H···P−O, as is ^3J(P,C) modulated by the angle C···P−O in this work. Latest bench mark calculations by Del Benne et al. carried out at the CCSD level of theory further support the strong dependence of both couplings on deviation from the linear arrangement of atoms along the motif.[20b]

The contribution of the FC term is always dominant for the ^3J(P,C) coupling (see Supporting Information). This is however not true for all grid point calculations of the ^2J(P,H) coupling. For example, when considering the angular dependence of the ^2J(P,H) coupling at the optimal R(P···C) distance, 4.52 Å, the FC term contributes by −5.3, −4.0, −0.4, 0.1, and 0.1 Hz for the C···P−O angle values 0°, 10°, 30°, 50°, and 90°, respectively. At the same time, the PSO term contributes by 1.3, 1.0, −0.2, −0.7, and −0.7 Hz; the DSO one, by 0.1, 0.1, 0.4, 0.6, and 0.7 Hz; and the SD term, by 0.8, 0.5, −0.1, 0.0, and 0.0 Hz for the same grid of the C···P−O angle. The interatomic distance R(O···H) spans the interval 1.93 ÷ 2.27 Å and 2.26 ÷ 3.75 Å for the C···P−O angle smaller and larger than 30°, respectively. In a nearly collinear arrangement of the P−O···H−C linkage, the PSO and SD terms put together form a notable positive contribution to the total ^2J(P,H) coupling that partially reduces the negative contribution of the FC term. In contrast, in an arrangement with the C···P−O angle larger than 30°, the total ^2J(P,H) coupling corresponds almost solely to the FC term due to the partial compensation of the DSO and PSO terms and negligible SD term. The accurate calculation of the ^2J(P,H) coupling constant thus requires inclusion of all four coupling contributions. Different behaviors of both couplings result in different limit values for the C···P−O angle close to 30°. While the limit for the ^3J(P,C) coupling is negative for all isosurfaces with constant R(P···C) distance, the ^2J(P,H) coupling is limited to zero being positive or negative dependent on the R(P···C) distance. This is shown in detail in Figure 3.

^3J(P,C) and ^2J(P,H) Couplings Calculated in Nucleotides of Ribosomal RNA. A favorable arrangement of the P−O···H−C link can in principle be intra- or internucleotide. The RNA nucleotides used for the present calculations correspond to the second case. They were selected from nucleotides of the 23S rRNA of the crystal structure of the large ribosomal unit.[22] To find some representative nucleotides that fit the geometry constraints revealed by the model calculations for the G···dmP complex, we performed a simple search for intranucleotide motifs with the P−O···H angle close to 180° and a minimal interatomic distance R(O···H). Sixteen such nucleotides with a large variability of their conformations were selected. These nucleotides are further identified by residue type and number as labeled in the ribosomal crystal structure.[22] Six of these nucleotides (G539, A632, G940, A1287, G1600, C2760) can be classified as noncanonical A-RNA conformations with alpha and gamma torsions in unusual regions but compensating each other (they correspond to RNA backbone families 24 and 27[6b]). Conformations of these nucleotides, while rare compared to the

(19) Mishima, M.; Hatanaka, M.; Yokoyama, S.; Ikegami, T.; Wälchli, M.; Ito, Y.; Shirakawa, M. *J. Am. Chem. Soc.* **2000**, *122*, 5883−5884.
(20) (a) Czernek, J.; Brüschweiler, R. *J. Am. Chem. Soc.* **2001**, *123*, 11079−11080. (b) Alkorta, I.; Elguero, J.; Del Bene, J. E. *Chem. Phys. Lett.* **2005**, *412*, 97−100.
(21) *MATLAB*, version 6.5.
(22) Ban, N.; Nissen, P.; Hansen, J.; Moore, P. B.; Steitz, T. A. *Science* **2000**, *289*, 905−920.

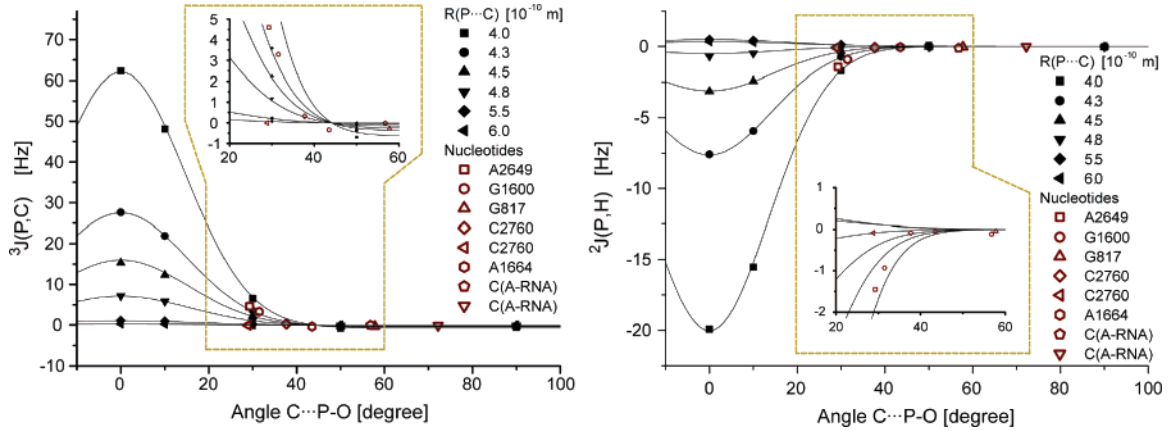

Figure 3. Calculated NMR spin−spin coupling constants ^3J(P,C) and ^2J(P,H) across the P−O···H−C link in the model complex G···dmP. The filled symbols correspond to the couplings of the grid point calculation at different R(P···C) distances fitted as described in the Appendix (see Supporting Information). The open symbols in red color correspond to the couplings in RNA nucleotides of Table 1.

Table 1. Calculated NMR Spin−Spin Coupling Constants ^3J(P,C) and ^2J(P,H) Across the P−O···H−C Motif in the Selected RNA Nucleotides

nucleotide[a]	$^3J(^{31}P,^{13}C)$[b]	$^2J(^{31}P,^1H)$[b]	R(P···C)[c]	R(O···H)[c]	α(C···P−O)[c]	α(P···C−H)[c]
A 2649 (C8−H8)	4.60	−1.45	4.2333	1.9731	29.3	16.5
G 1600 (C8−H8)	3.29	−0.93	4.3889	2.1322	31.5	9.3
G 817 (C8−H8)	−0.29	−0.04	4.2650	2.8239	57.8	38.1
C 2760 (C6−H6)	0.32	−0.12	4.9038	2.7410	37.7	11.5
C 2760 (C5−H5)	−0.01	0.08	5.8248	4.3733	28.9	80.1
A 1664 (C8−H8)	−0.27	−0.16	3.8757	1.9371	43.5	12.1
C[d] (C6−H6)	−0.02	−0.11	4.2779	3.2652	56.8	63.5
C[d] (C5−H5)	−0.08	−0.01	4.8310	3.5528	72.2	18.6

[a] RNA nucleotides (A, adenosine-5′-phosphate; G, guanosine-5′-phosphate; C, cytosine-5′-phosphate) with the residue number taken from the 23S rRNA of the 50S ribosomal unit.[22] The C−H bond considered in the calculations is indicated in parentheses. [b] Calculated NMR spin−spin coupling constant [Hz]. [c] Internuclear distance R [Å], bond angle α [deg]. [d] Canonical A-RNA conformation.

canonical A-RNA, have been observed in the 23S rRNA[22] quite frequently and the possibility of their identification by measuring their ^3J(P,C) and ^2J(P,H) NMR coupling constants is significant. Next three nucleotides (G817, A174, A1369) are in an unusual but well defined conformational family forming non-Watson−Crick base pairs in purine-rich regions of double helices (this conformation is labeled as number 5[6b]). The remaining residues (U200, A1664, C1692, A2074, G2092, A2649, C2850) have unusual conformations that are currently not classified.

Actual calculation of the indirect spin−spin couplings was performed for six representative nucleotides from the above set of 16 as well as for the canonical A-RNA conformation to put the calculation into a context of the most common RNA conformation. The calculated ^3J(P,C) and ^2J(P,H) coupling constants are listed together with the geometry parameters for selected nucleotides in Table 1. Nucleotide A2649 has the geometry of the P−O···H−C link most favorable for effective spin−spin interaction, G817 is an example of a non-A-RNA conformation (labeled as conformation number 5 [6b]), and G1600 and C2760 are both modified A-type conformations (labeled as conformation number 24[6b]); C2760 is also a pyrimidine nucleotide with two possible contacts between the phosphate and H5−C5 or H6−C6 group of the pyrimidine base. Nucleotide A1664 was selected for the NMR calculation because it is an important part of the reverse kink-turn as observed in helix 54 of the ribosomal structure.[22]

A dramatic geometry variation of the P−O···H−C motif dictated by variation of the overall RNA structure offers a possibility of using this motif as an NMR probe for less frequently populated RNA conformations. For instance, the above-mentioned reverse kink-turn motif is a newly discovered RNA structural and possibly also functional motif. It is an elbowlike helix−loop−helix motif, first observed within the group I intron.[23] Its sequence resembles the more common elbowlike "regular" kink-turns,[7a] but it bends in the opposite direction, toward the major groove of the flanking helices. A possibility of identifying a signal distinct for a residue in the actual turn of this motif, exemplified here by residue A1664, represents a new route to its structural identification.

The calculated spin−spin coupling constants ^3J(P,C) and ^2J(P,H) are shown in Table 1. Sizable NMR couplings were calculated for the nucleotides A2649 and G1600 shown in Figure 4. In both nucleotides, the angles C···P−O and P···C−H show small deviations from the linear arrangement, and the mutual arrangement of the phosphate group and base effectively conveys the spin−spin interaction across the P···C link. The calculated NMR spin−spin couplings are also modulated by the interatomic distances R(P···C) and R(O···H). While the angles listed in Table 1 for nucleotides A2649 and G1600 are almost the same, both R(P···C) and R(O···H) distances are shorter by about 0.15 Å in nucleotide A2649. The coupling constant ^3J(P,C) is correspondingly larger, by 1.3 Hz, in nucleotide A2649. A similar trend can also be seen for the negative coupling ^2J(P,H). The C···P−O angle in these nucleotides roughly corresponds to 30°, corresponding to the ^3J(P,C)

(23) (a) Adams, P. L.; Stahley, M. R.; Gill, M. L.; Kosek, A. B.; Wang, J. M.; Strobel, S. A. *RNA* **2004**, *10*, 1867−1887. (b) Strobel, S. A.; Adams, P. L.; Stahley, M. R.; Wang, J. M. *RNA* **2004**, *10*, 1852−1854.

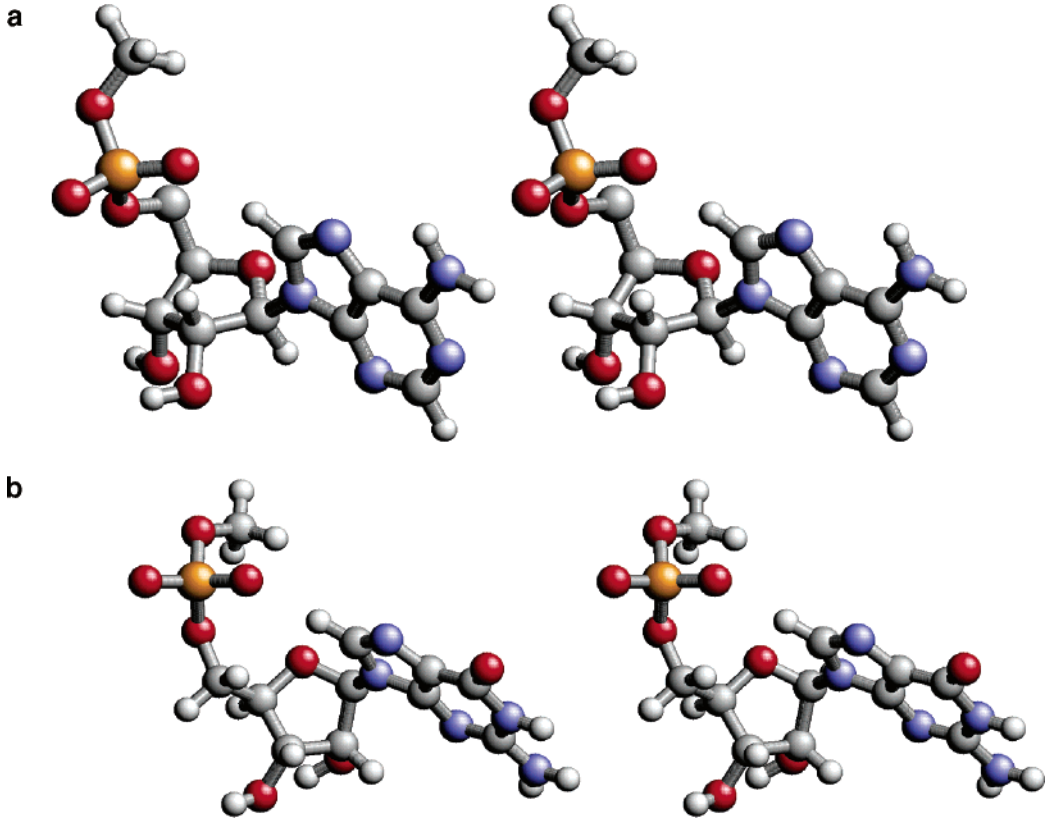

Figure 4. Stereoview of nucleotides A2649 (a) and G1600 (b) of the large ribosomal subunit (Ban et al. *Science*, **2000**, *289*, 905).

Table 2. Individual Contributions of the Coupling Constants ^3J(P,C) and ^2J(P,H) Calculated in the Selected RNA Nucleotides at Different Levels of Theory

	$^3J(^{31}P,^{13}C)$[a]		$^2J(^{31}P,^{1}H)$[a]	
nucleotide[b]	Iglo II	Iglo III	Iglo II	Iglo III
A 2649 (C8−H8)	4.60 (0.08, −0.03, 4.58, −0.01)	4.43 (0.08, −0.04, 4.41, −0.02)	−1.45 (0.45, 0.08, −1.94, −0.05)	−1.41 (0.46, 0.06, −1.88, −0.05)
G 1600 (C8−H8)	3.29 (0.07, −0.05, 3.27, 0.02)	3.19 (0.07, −0.05, 3.17, 0.00)	−0.93 (0.48, −0.25, −1.09, −0.06)	−0.95 (0.49, −0.28, −1.09, −0.07)
G 817 (C8−H8)	−0.29 (0.09, −0.10, −0.29, −0.01)	−0.28 (0.09, −0.11, −0.26, −0.01)	−0.04 (0.62, −0.69, 0.08, −0.04)	−0.11 (0.62, −0.75, 0.06, −0.04)
C 2760 (C6−H6)	0.32 (0.05, −0.04, 0.31, 0.00)	0.33 (0.05, −0.05, 0.32, 0.00)	−0.08 (0.44, −0.38, −0.11, −0.03)	−0.13 (0.44, −0.41, −0.13, −0.03)
C 2760 (C5−H5)	−0.01 (0.00, 0.00, −0.02, 0.00)	−0.01 (0.00, 0.00, −0.02, 0.00)	0.08 (0.04, 0.02, 0.00, 0.02)	0.08 (0.04, 0.02, 0.01, 0.02)
A 1664 (C8−H8)	−0.27 (0.11, −0.11, −0.26, 0.00)	−0.14 (0.11, −0.12, −0.12, 0.00)	−0.16 (0.88, −1.05, 0.11, −0.09)	−0.20 (0.89, −1.11, 0.12, 0.00)

[a] Individual contributions in parentheses (diamagnatic spin−orbit, paramagnetic spin−orbit, Fermi-contact, spin−dipolar) calculated with atomic basis Iglo II and Iglo III. [b] RNA nucleotides (A, adenosine-5′-phosphate; G, guanosine-5′-phosphate; C, cytosine-5′-phosphate) with the residue number taken from the 23S rRNA of the 50S ribosomal unit.[22] The C−H bond considered in the calculations is indicated in parentheses.

coupling 6.5, 2.6, and 2.2 Hz when calculated in the model complex G···dmP with the R(P···C) distance equal to 4.0, 4.3, and 4.5 Å, respectively. The calculated coupling constants in the real structure of nucleotide A2649 and G1600 fit well to the prediction by model calculations as shown in detail in Figure 3 when the couplings of both nucleotides are very close to the curve corresponding to distance R(P···C) ≈ 4.3 Å. The ^3J(P,C) coupling fitted by the function described in the Appendix was 4.44, 2.23, −0.37, 0.23, and 0.11 Hz for the A2649, G1600, G817, and C2760 nucleotides, respectively. This good qualitative agreement of the values calculated with the quantum chemical approach shown in Table 1 and the numerical fit validates the use of the fitted function for the prediction of the couplings in the P−O···H−C motifs.

The performance of different atomic basis on calculated spin−spin couplings is shown in Table 2. The magnitude of the ^3J(P,C) coupling is slightly smaller when the atomic basis Iglo III was used; a maximal difference of 0.17 Hz was obtained for the nucleotide A2649 when calculated with the Iglo II and Iglo III basis. Separation of calculated ^3J(P,C) couplings into the individual contributions unveils the dominant dependence on atomic basis for the Fermi-contact contribution that is in agreement with the finding for the grid point calculation. The magnitude of the ^2J(P,H) couplings in Table 2 changes less than 0.07 Hz. The effect of water solvent was calculated only for the nucleotide A2649 with the Iglo III basis; the ^3J(P,C) and ^2J(P,H) couplings were 4.55 and −1.37 Hz, respectively. The

water solvent thus affects the magnitude of both couplings similar to the size of atomic basis.

A key importance of the mutual collinearity of P−O and H−C bonds becomes apparent when comparing the sizable spin−spin couplings calculated in nucleotides A2649 and G1600 with those calculated in nucleotide G817. Although the interatomic distance *R*(P···C) is shorter in nucleotide G817 than in G1600, substantially larger angles C···P−O and P···C−H in G817 result in damping of both spin−spin couplings. On the other hand, the distance *R*(P···C6) is larger in nucleotide C2760 than in G817 by 0.64 Å, but a significantly more collinear arrangement between the P−O and H−C bonds in C2760 results in a larger value of the ^3J(P,C) coupling. This is again in agreement with the strong angular dependence of both spin−spin couplings revealed by the model calculation shown in Figure 3. NMR calculation for the selected nucleotides as well as for the G··· dmP model shows that once the C···P−O or P···C−H angle becomes larger than 50°, both investigated NMR couplings drop to zero.

The angular arrangement of atoms in the P−O···H−C linkage dominates the values of the calculated couplings. For instance, the angles listed in Table 1 for nucleotides A1664 and C2760 (C6−H6) are similar and despite the tighter packing of the phosphate to the base in A1664 than in C2760, the $|^3J(P,C)|$ coupling is similar in both nucleotides. As a rule of thumb, the model grid point calculations suggest that the angle C···P−O corresponding roughly to 40° symbolizes the borderline between the couplings with magnitudes larger or smaller than 1 Hz.

In canonical A-RNA, the P−O···H−C link is too nonlinear and also the interatomic distance R(P···C) is relatively large as shown in Table 1. The indirect NMR spin−spin couplings are therefore negligible in this dominating RNA conformation.

Conclusions

The NMR spin−spin coupling constants ^3J(P,C) and ^2J(P,H) across the P−O···H−C intranucleotide link in nucleic acids exhibit strong dependence on the mutual angular orientation between the P−O phosphate bond and the H−C bond in a base. The indirect NMR spin−spin couplings depend strongly on the overall arrangement of the motif; the linear arrangement of P−O···H−C atoms and the short distance between the P−O and H−C moieties is the prerequisite for a sizable value of NMR couplings, similar to what was found also for the analogous motifs.[13,20]

According to our calculations, a deviation from the linear arrangement of either the C···P−O or P···C−H angle larger than ∼50° results in negligible NMR spin−spin interaction and the value $|J|$ approaches zero rapidly for both indirect couplings. The coupling constants with $|J| > 1$ Hz can be on the other hand expected for the confined interval of the bond angles smaller than ∼50° leading to the relatively narrow P−O···H−C link.

Inclusion of implicit water solvent as modeled by PCM has only a small effect on calculated values of both couplings. The indirect coupling ^3J(C,P) is dominated by the Fermi-contact type of spin−spin interaction. For the ^2J(H,P) coupling, all four terms contribute indispensably, especially in the nearly collinear arrangement of the P−O···H−C linkage.

Measurable values of indirect spin−spin couplings can be expected only for quite specific structural arrangements of ribonucleotides. Critical is especially a linear arrangement of the P−O bond in the phosphate relative to the H−C bond of a base.

Reliable theoretical modeling of indirect spin−spin couplings across the P−O···H−C linkage can be used for determination and validation of structural motifs and tertiary contacts in nucleic acids, nucleic acid/protein, and nucleic acid/drug complexes which are difficult or impossible to detect by other means. The present results suggest that the indirect spin−spin couplings across the P−O···H−C motif, although negligible for most RNA architecture types, could help detect some distinct backbone topologies, as seen for example in the reverse kink-turn.

Acknowledgment. This study has been supported by the Grant Agency of the Czech Republic 203/05/0388.

Supporting Information Available: Individual contributions of the indirect spin−spin coupling constants calculated for the ^3J(P,C) and ^2J(P,H) couplings of the grid point calculation, Cartesian coordinates of selected nucleotides, complete ref 18, and Appendix. This material is available free of charge via the Internet at http://pubs.acs.org.

JA0551180